Functional photoacoustic microscopy in vivo

Hao F. Zhang, Konstantin Maslov, Jung-Taek Oh, George Stoica, Lihong V. Wang

Hao F. Zhang, Konstantin Maslov, Jung-Taek Oh, George Stoica, Lihong V. Wang, "Functional photoacoustic microscopy in vivo," Proc. SPIE 6086, Photons Plus Ultrasound: Imaging and Sensing 2006: The Seventh Conference on Biomedical Thermoacoustics, Optoacoustics, and Acousto-optics, 60861G (6 March 2006); doi: 10.1117/12.645143

SPIE.

Event: SPIE BiOS, 2006, San Jose, California, United States

Functional photoacoustic microscopy *in vivo*

Hao F. Zhang[a], Konstantin Maslov[a], Jung-Taek Oh[a], George Stoica[b], Lihong V. Wang[a]*
[a]Dept. of Biomedical Engineering, Texas A&M University, College Station, TX, USA 77843-3120;
[b]Dept. of Veterinary Pathobiology, Texas A&M University, College Station, TX, USA 77843-5547

ABSTRACT

Functional photoacoustic microscopy is a hybrid imaging technique that detects laser induced photoacoustic waves to image biological tissues in three dimensions. Its imaging depth exceeds the fundamental depth limit of the existing high resolution optical imaging modalities while maintaining a comparable ratio of imaging depth to axial resolution. The amplitude of photoacoutic waves is related to tissue's optical absorption and, therefore, functional imaging can be achieved by acquiring spectroscopic information. We demonstrate here the capabilities of functional photoacoustic microscopy by volumetric imaging a skin melanoma tumor and functional imaging of hemoglobin oxygen saturation in single vessels *in vivo.*

Keywords: Photoacoustic, microscopy, melanoma, hemoglobin, oxygenation

1. INTRODUCTION

How to image deep biological tissues with high spatial resolution still remains challenging in optical imaging. Current high-resolution optical imaging modalities, which can be defined as having a ratio of maximum imaging depth to axial resolution greater than 100, include confocal microscopy[1], two-photon microscopy[2], and optical coherence tomography[3]. They rely on the detection of unscattered or singly backscattered (ballistic or quasiballistic) photons to provide high spatial resolution. Therefore, the imaging depth is fundamentally limited to approximately 1 mm in highly scattering biological tissues, which is related to the optical transport mean free path. Beyond this depth, photons are multiply scattered (diffused) and no existing optical imaging technique can detect them with high spatial resolution.

Unlike pure optical imaging techniques, functional photoacoustic microscopy (fPAM) detects diffuse photons indirectly. It detects the absorbed diffuse photons ultrasonically in tissue through photoacoustic (PA) effect[4].

When short-pulsed laser irradiates biological tissues, wideband ultrasonic waves (referred to as PA waves) are induced as a result of the transient thermoelastic expansion inside the tissue. Because ultrasonic scattering is 2-3 orders of magnitude weaker than optical scattering[5], high-frequency ultrasonic imaging provides better spatial resolution in deep biological tissues than existing optical imaging. Therefore, the optical absorbers, from where PA waves are generated, can be localized at high resolution beyond the abovementioned depth limit by using a focused high-frequency ultrasonic transducer. Since absorbed photons produce PA waves regardless of their scattering status, fPAM can penetrate more deeply by taking advantage of diffuse photons.

The magnitude of the PA waves is proportional to the local optical energy deposition and, therefore, fPAM images the internal optical absorption distribution of tissues. When the wavelength of irradiating laser varies, the amplitude of the PA waves will change according to the absorber's extinction coefficient. Since optical absorption is strongly related to the molecular conformation and concentration, fPAM is able to extract functional parameters based on spectral measurement. In comparison, all the abovementioned high-resolution optical imaging modalities are insensitive to the physiologically specific optical absorption contrast.

Due to ultrasonic localization, the lateral resolution of fPAM is determined by the ultrasonic focal diameter, and the axial resolution is inversely related to the bandwidth of the ultrasonic transducer. Similar to traditional ultrasonic microscopy, the diffraction-limited lateral resolution of fPAM can be expressed as $0.61v/(f\mathrm{NA})$, where v is the sound

* lwang@tamu.edu; phone: 1 979 847-9040; fax: 1 979 845-4450; oilab.tamu.edu

Photons Plus Ultrasound: Imaging and Sensing 2006: The 7th Conference on Biomedical Thermoacoustics, Optoacoustics, and Acousto-optics, edited by A. A. Oraevsky, et. al
Proc. of SPIE Vol. 6086, 60861G (2006) • 1605-7422/06/$15 • doi: 10.1117/12.645143

velocity, *f* and NA are the central frequency and the numerical aperture of the ultrasonic detector, respectively. Therefore, fPAM requires a wideband, high frequency, and large NA ultrasonic transducer to achieve high spatial resolution. Because of strong frequency-dependent acoustic attenuation at central frequencies higher than 10 MHz, the maximum imaging depth of fPAM is limited by the ultrasonic penetration depth, rather than the optical penetration depth of the diffuse photons. As a result, the axial resolution, the lateral resolution, and the imaging depth of fPAM are all scaleable with the ultrasonic parameters within the reach of diffuse photons.

Within the visible spectral region, fPAM is highly sensitive to deoxyhemoglobin (HbR), oxyhemoglobin (HbO_2), and melanin, because of their high optical absorption. Here we demonstrate the capabilities of fPAM through (1) the volumetric imaging of skin melanoma tumor as well as its surrounding blood vessels *in vivo*; and (2) the functional imaging of hemoglobin oxygen saturation (SO_2) in single blood vessels *in vivo*.

2. EXPERIMENTAL SETUP

The schematic diagram of the fPAM is shown in Fig. 1. We used a Nd:YAG laser (repetition rate: 10 Hz; pulse width: 6.5 ns; wavelength: 532 nm at second harmonic) pumped tunable dye laser as the irradiation source. Laser light (wavelength range: 570-770 nm) was delivered through an optical fiber and expanded by a conical lens to form an annular beam. Light was then weakly focused into the tissue with its focal region overlapping the ultrasonic focus coaxially. The optical illumination was ring-shaped with a dark center so that no strong PA signals were produced from the skin surface, which prevented the reverberation from shadowing signals from deep structures. The energy density deposited on the skin surface was kept well within the ANSI safety limit in our spectral range (20 mJ/cm^2)[6]. The PA waves were detected by an ultrasonic transducer (central frequency: 50 MHz; nominal bandwidth: 70%; NA: 0.5) for 2 μs at each transducer location. They were digitized by an oscilloscope working at a 250-MHz sampling rate without signal averaging. The one-dimensional time-resolved PA signals were converted into depth-resolved images based on the sound velocity in soft tissue (1.54 mm/μs). The components within the dashed-box in Fig. 1 were raster scanned together in the *x-y* plane with a step size of 50 μm to acquire a volumetric image. The motion controller, which was synchronized by the triggering signal from the Nd:YAG laser, also controlled the tunable dye laser to change optical wavelength automatically during spectral measurements.

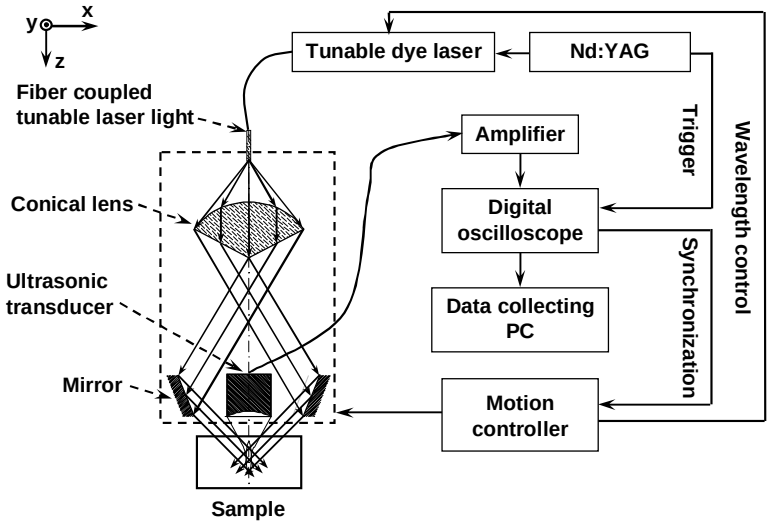

Fig. 1. Schematic of the fPAM system.

The point spread function was acquired by imaging a carbon fiber with a diameter of 6 μm, and the lateral and axial resolutions of this fPAM were quantified to be 45 μm and 15 μm, respectively[7]. The maximum imaging depth of fPAM was measured to be more than 3 mm in live animal. As a result, fPAM has a depth-to-resolution ratio greater than 100.

3. RESULTS AND DISCUSSION

3.1 Volumetric imaging of skin melanoma tumor and it surrounding vasculature

We imaged a subcutaneously inoculated B16 melanoma in an immunocompromised nude mouse (body weight: 20 g). Two optical wavelengths (584 and 764 nm) were used in this experiment. Using visible light (584 nm), fPAM can image both the melanoma and the surrounding blood vessels in the *x*-*y* plane due to the comparably strong optical absorption of both melanin and hemoglobin. However, tumor thickness cannot be evaluated within this wavelength range because light is completely absorbed by the melanin-rich tumor within a very short optical penetration depth. In order to penetrate through the tumor, near-infrared light (764 nm) was employed as a result of the decreased optical absorption of melanin. Therefore, a combination of the images from these two optical wavelengths reveals the complete volumetric morphology of the melanoma tumor and its surrounding blood vessels.

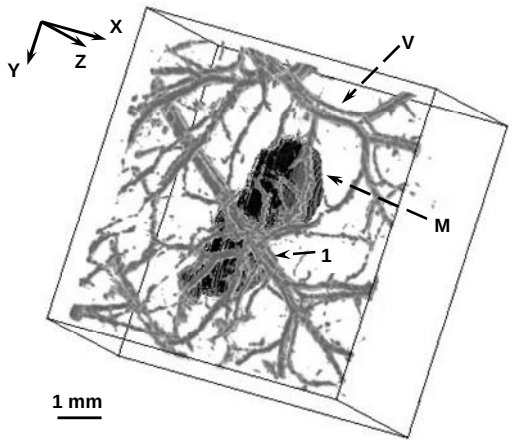

Fig 2. Volumetric imaging of a melanoma tumor and its surrounding blood vessels *in vivo*. The blood vessels (V) and the melanoma (M) are visualized in different grayscales based on images acquired from 584-nm and 764-nm wavelengths, respectively. Two blood vessels (numbered by 1) can be observed running in parallel at different depths above the melanoma tumor. In this particular case, the melanoma tumor is below the vessel network. The displayed volume covers 8 mm along the *x* and *y* axes and 1.2 mm along the *z* axis, where the 1.2-mm is magnified 4 times for clarity.

Figure 2 demonstrates the high spatial resolution and high contrast of fPAM. Up to 6 orders of vessel branching can be observed and the imaged smallest blood vessel has a diameter less than 0.05 mm, which only occupies a single pixel in the *x*-*y* plane. Higher density of small blood vessels directly on top of the tumor is clearly observed, which, presumably, is resulted from angiogenesis. The average ratio of blood vessels to the background in PA signal amplitude is 13±0.9 at the 584-nm wavelength. The average ratio of melanoma to blood vessels is 0.9±0.02 at the 584-nm wavelength and as high as 29±3 at the 764-nm wavelength. This high image contrast is resulted from the strong optical absorption of hemoglobin and melanin and minimal tissue absorption.

The thickness of skin melanoma is the sole key parameter for both diagnosis and prognosis purposes, however it is not being measured correctly using existing noninvasive methods[8]. In Fig. 2, the measured thickness of the melanoma is 0.3 mm and the depth of the tumor is 0.32 mm from the skin surface. Based on its high specificity in imaging melanin at the 764-nm wavelength, fPAM can potentially be used to provide critical information for the clinical diagnosis and prognosis of melanoma.

Figure 2 also indicates that fPAM can be used to image tumor angiogenesis in the early stages based on its high contrast and high spatial resolution. The imaging of angiogenesis is invaluable for understanding tumor growth and metastasis[9]. However, no existing methods are capable of imaging the microvasculature of tumors in natural conditions *in vivo* without the help from an extrinsic contrast agent so far.

3.2 Functional imaging of SO_2 in single blood vessels

The SO_2 was imaged in subcutaneous blood vessels in a Sprague Dawley rat (body weight: 200 g) under normoxia condition. In functional imaging of SO_2, fPAM treats HbR and HbO_2 as the dominant optical absorbers and calculates their relative concentrations based on their molar extinction spectra and a spectral measurement, which is in the same manner as near infrared spectroscopy (NIRS)[10] does. However, NIRS measures only volume-averaged SO_2, whereas fPAM can pinpoint individual blood vessels and can evaluate their local SO_2 by taking advantage of the high resolution ultrasonic localization., In an *ex vivo* bovine blood study, the measured SO_2 values from fPAM showed agreement with results from the standard optical method[11] with a relative systematic difference of less than 4%.

In the *in vivo* animal experiment, we used PA singles acquired from four different wavelengths (578, 584, 590, and 596 nm) to calculate SO_2 based on a least-squares fitting (Fig. 3). Since HbR and HbO_2 have identical molar extinction coefficient at the 584-nm wavelength (isosbestic point), the amplitude of PA waves reflects the total hemoglobin concentration distribution regardless of the oxygenation status of hemoglobin as shown in Fig. 3(A).

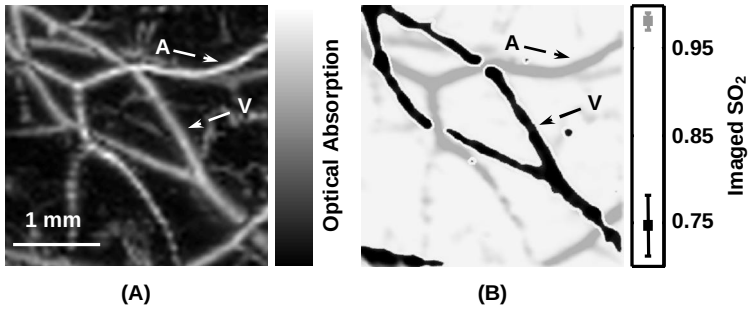

Fig. 3. Functional imaging of SO_2 *in vivo*. (A) A structural image acquired at the 584-nm optical wavelength. The maximum intensity of the PA signal at each location of the ultrasonic detector was projected onto the *x-y* plane to form this two-dimensional image. (B) A vessel-by-vessel SO_2 mapping. A: arteriole; V: venule.

In Fig. 3(B), the imaged SO_2 measures approximately 0.98±0.01 in arterial blood and 0.74±0.03 in venous blood. Each single vessel was categorized as either an arteriole or venule based on the imaged SO_2 values, which was further verified by results from a modified double-dye[12] injection method and histology. fPAM was also successfully used to monitor the dynamic variations of SO_2 when physiological state alters, which indicated that fPAM can be applied to study brain functions based on the local deoxygenation after intensive neuron firing[13]. By tuning optical wavelengths toward other endogenous pigments or administered contrast agents, fPAM can also be adapted to other applications such as molecular imaging.

4. SUMMARY

In summary, fPAM is a non-invasive imaging modality that can image biological tissue in three dimensions *in vivo*. It extends the fundamental depth limit of the existing high-resolution optical imaging modalities while maintaining a high depth-to-resolution ratio. Based on optical absorption contrast, fPAM can achieve functional imaging with high contrast, sensitivity and specificity by choosing suitable working optical wavelengths and performing spectral measurements. Moreover, the tunability of optical wavelength and the scalability of spatial resolution and imaging depth of fPAM provide great flexibility for different imaging purposes.

ACKNOWLEDGES

We thank Ovidiu Craciun, Geng Ku, Meng-lin Li, and Gina Lungu for experimental assistance. This project is sponsored by National Institutes of Health grants R01 EB000712 and R01 NS46214.

REFERENCES

[1] T. Wilson, and C. Sheppard, *Theory and Practice of Scanning Optical Microscopy*, Academic Press, London, 1984.
[2] W. Denk, J. H. Strickler, and W. W. Webb, "Two-photon laser scanning fluorescence microscopy," Science **248**, 73-76 (1990).

[3] D. Huang *et al.*, "Optical coherence tomography," Science **254**, 1178-1181 (1991).
[4] T. Sun, and G. J. Diebold, "Generation of ultrasonic waves from a layered photoacoustic source," Nature **355**, 806-808 (1992).
[5] F. A. Duck, *Physical Properties of Tissue,* Academic Press, London, 1990.
[6] *American national standard for the safe use of lasers Z136.1,* American National Standards Institute, New York, 2000.
[7] K. Maslov, G. Stoica, and L. V. Wang, "*In vivo* dark-field reflection-mode photoacoustic microscopy," Opt. Lett. **30**, 625-627 (2005).
[8] E. Ruocco, G. Argenziano, G. Pellacani, and S. Seidenari, "Noninvasive imaging of skin tumors," Dermatological Surgery **30**, 301-310 (2004).
[9] P. Carmeliet, and R. K. Jain, "Angiogenesis in cancer and other diseases," Nature **407**, 249 (2000).
[10] J. S. Wyatt, D. T. Delpy, M. Cope, S. Wray, and E. O. R. Reynolds, **"**Quantification of cerebral oxygenation and hemodynamics in sick newborn-infants by near-infrared spectrophotometry," Lancet **2**, 1063-1066 (1986).
[11] M. U. Tsao, S. S. Sethna, C. H. Sloan, and L. J. Wyngarden, "Spectrophotometric determination of the oxygen saturation of whole blood," J. Biol. Chem. **217**, 479-487 (1955).
[12] G. Ambach, and M. Palkovits, "Blood supply of the rat hypothalamus I. nucleus supraopticus," ACTA Morphol. Acad. Sci. Hung. **22**, 291-310 (1974).
[13] I. Vanzetta, and A. Grinvald, ˝Increased cortical oxidative metabolism due to sensory stimulation: implications for functional brain imaging,˝ Science **286**, 1555-1558 (1999).